Iran J Public Health, Vol. 54, No.5, May 2025, pp.1074-1086

Original Article

Increased Expression of *RCN1P2*, *TPM3P9*, and *HSP90AB3P* as Non-Coding RNA in Gastric Cancer Linked to Proliferative, Inflammatory and Metastatic Pathways through a Competing Endogenous RNAs Network

Ensieh Sagheb Sadeghi [1,2], ***Zahra Amrollahy Bioky*** [2,3], ***Mahsa Hokmabadi*** [2,4], ***Samira Asadollahi*** [2,5], ***Fatemeh Sarhadi*** [2,6], ***Nasrin Fattahi Dolatabadi*** [2], ***Atefeh Zamani*** [2], ****Mohammad Mahdevar*** [7], ****Maryam Peymani*** [8]

1. *Department of Biology, Neyshabur Branch, Islamic Azad University, Neyshabur, Iran*
2. *Gene Raz Bu Ali, Genetic and Biotechnology Academy, Isfahan, Iran*
3. *Department of Animal Biology, Faculty of Natural Sciences, University of Tabriz, Tabriz, Iran*
4. *Department of Genetic, Tehran Medical Sciences Branch, Islamic Azad University, Tehran, Iran*
5. *Research Center for Food Hygiene and Safety, Shahid Sadoughi University of Medical Sciences, Yazd, Iran*
6. *Department of Biology, Medical Biotechnology Research Center, Ashkezar Branch, Islamic Azad University, Ashkezar, Yazd, Iran*
7. *Department of Genetics and Molecular Biology, School of Medicine, Isfahan University of Medical Sciences, Isfahan, Iran*
8. *Department of Biology, Faculty of Basic Sciences, Shahrekord Branch, Islamic Azad University, Shahrekord, Iran*

***Corresponding Authors:** Emails: m.peymani@iaushk.ac.ir, mahdevar416@gmail.com

(Received 15 Mar 2024; accepted 10 Jun 2024)

Abstract

Background: This study aimed to find pseudogenes with significant expression alterations in gastric cancer (GC) that could be implicated in the disease's development via the competing endogenous RNAs (ceRNAs) network.

Methods: Pseudogenes, mRNAs, and microRNAs, whose expression changes considerably in GC specimens, were identified using the Cancer Genome Atlas (TCGA) data from 2006 to 2017 (USA). The ceRNAs network was constructed using the miRWalk, miRTarBase, and DIANA-LncBase. The cox regression test was performed to assess the correlation between candidate genes and patient prognosis. Finally, using the RT-qPCR method, the in-silico results were evaluated using GC samples and adjacent normal. Samples were collected from Imam Khomeini Hospital in Tehran (Iran) between 2020 and 2021.

Results: In the cancer samples compared to the normal ones, there were 86 miRNAs, 1985 mRNAs, and 33 pseudogenes showing expression alterations, either more than or less than a twofold difference**.** Constructed ceRNA network demonstrated that pseudogenes such as *RCN1P2*, *TPM3P9*, and *HSP90AB3P* were most connected to changed mRNAs and microRNAs in GC. The analysis of the ceRNA network for each of the mentioned pseudogenes indicated that the associated mRNAs play roles in cell proliferation, inflammation, and metastatic pathways. Furthermore, elevated expression of several mRNAs linked to potential pseudogenes was linked to a poor prognosis. RT-qPCR revealed a significant increase in the expression levels of *RCN1P2*, *TPM3P9*, and *HSP90AB3P* in GC samples.

Conclusion: The expression of *RCN1P2*, *TPM3P9*, and *HSP90AB3P* is dramatically enhanced in GC. They can also influence the survival rate of GC patients by regulating pathways involved in cell proliferation, inflammation, and metastasis via the ceRNAs network.

Keywords: Gene expression; ceRNAs network; MicroRNAs; Pseudogenes

DOI: https://doi.org/10.18502/ijph.v54i5.18642

Introduction

In 2020, gastric cancer (GC) was one of the most frequent malignancies, and it had a poor survival rate (1). The expression of many genes changes as a disease progresses and that these changes are linked to malignancy and patient survival rates (2-4). Changes in gene expression have also been linked to drug resistance and sensitivities, according to research (5, 6).

Pseudogenes are a type of non-coding gene that was once thought to be junk DNA (7). However, with the aid of next-generation sequencing and research advance in non-coding RNAs, multi-layered functions of pseudogenic DNA, RNA, or protein have been discovered in multiple cancer (8). *POU5F1B* a processed pseudogene that is highly homologous to *OCT4*, is increased in GC samples and can dramatically increase malignancy in GC cell lines (9). *PTENP1* is reduced in GC and can act as a tumor suppressor by inhibiting GC cell lines' invasion, proliferation, and apoptosis (10). Furthermore, numerous investigations have revealed that the expression of various pseudogenes in the GC is altered and that their expression is linked to malignancy and GC development (9, 11, 12). On the other hand, pseudogenes in a variety of malignancies, including GC, can regulate the expression of cancer-related genes via sponge microRNAs (miRNAs) and membership in the competing endogenous RNAs (ceRNAs) network (13, 14).

We aimed to find pseudogenes that regulate the expression of mRNAs involved in GC development through the ceRNAs network and whose expression patterns in GC samples are considerably different from normal.

Materials and Methods

Data source

GC transcriptome data (TCGA-STAD) from 2006 to 2017 (USA) in raw format (HTseq-Counts) was downloaded using the TCGAbiolinks package. Then, genes with zero or near-zero expression based on CPM criteria less than 10% in 70% of the samples were removed by the edgeR package. In the next step, data normalization based on the TMM method was applied on the data. The obtained expression matrix was used for the process of all analyzes. Moreover, the latest update of clinical information for all samples was downloaded and used for the analysis process. In the expression matrix for mRNAs and pseudogenes, the number of cancerous and normal samples were 375 and 32, respectively. On the other hand, in the expression matrix for miRNAs, the number of cancer and normal samples were 446 and 45 samples, respectively.

Identification of differentially expressed mRNAs, miRNA and pseudogenes

The expression difference between the groups was analyzed using the linear model approach, and the criteria $|logFC|>1$ and $FDR<0.01$ were used for gene selection. The BoMart tool (www.ensembl.org/biomart) was used to retrieve gene lists and information for mRNA and pseudogenes. Using the Enhanced Volcano package, expression changes were also visualized using volcano diagrams.

CeRNA network construct

Pseudogenes, mRNA, and miRNA with significant differences in expression were used to construct the ceRNA network. The miRWalk (mirwalk.umm.uni-heidelberg.de) and miRTarBase (mirtarbase.cuhk.edu.cn) databases were used to evaluate the relationship between miRNAs and mRNAs, and miRNA-mRNAs were selected that were validated by both databases. The DIANA-LncBase v3 (diana.e-ce.uth.gr/lncbasev3) database was employed for miRNA-pseudogenes interaction and validation type=direct, miRNA Conf.level=high and species=human were considered. The data were then integrated using the Cytoscape tool to construct the ceRNA network, and the degree>12 criterion was used to select key pseudogenes in the ceRNA network. The mentioned criterion was applied based on the

number of degrees of all pseudogenes and their median calculation.

Subnet and enrichment

Subnet networks were created using the Cytoscape tool to explore the connection of each candidate pseudogene with other miRNAs and mRNAs. The Enrichr database (maayanlab.cloud/Enrichr) and the MSigDB repository were utilized to enrich the data by using mRNAs from each network.

Preprocessing of clinical data and prognosis

The connection between the expression of candidate genes and the prognosis of patients with GC was investigated using TCGA-STAD clinical data. During the initial preprocessing of clinical data, normal specimens, specimens with a single day of living or NA, and specimens without a tumor at the time of death were excluded. The univariate Cox regression test was employed to look into the link between candidate gene expression and patient prognosis. The results were also confirmed using a Kaplan-Meier plot, and the median expression of identified genes was taken as a cut off.

Sample Collection

Twenty samples of GC along with 20 adjacent normal samples were obtained from the Tumor Bank of Iran. All cases of bioethics were reviewed and approved by the review board of Imam Khomeini Hospital (sample collection place) according to the criteria of the Ministry of Health, Treatment and Medical Education of Iran (Ethics Code: IR.IAU.TNB.REC.1400.005). In addition, a pathologist confirmed the illness state of all cancer samples, and their clinical information is described in Table 1. Samples were collected from Imam Khomeini Hospital in Tehran (Iran) between 2020 and 2021.

Table 1: Clinical information for GC

Characteristic	Number (N=20)
Age(yr)	
<50	6
>50	14
Gender	
Male	12
Female	8
TNM stage	
I	4
II	8
III	5
IV	3
Tumor size	
<5cm	9
>5cm	11

RNA extraction, cDNA synthesis and RT-qPCR

RNA was extracted using TRIzol (Invitrogen) according to the manufacturer's instructions. Then, DNase treatment (Sinaclon) was performed to remove DNA contamination. The cDNA was then synthesized using the Yektatajheiz kit. Specific primers for *RCN1P2* (F: 3'- CAACCAGAGCTTCCAGTACGA-5' and R: 3'-ACAATCTTCCCTAGCCTCTCCT-5'), *TPM3P9* (F: 3'-CACCGCGGCGCAGAGG-5' and R: 3'-GCTTCACTGCCTCGATGGTGG-5') and *HSP90AB3P* (F: 3'-CATGGAGAGGAGGAGGTGGAG-5' and R: 3'- TTGAAGGGTCTGTCAGGCTCT-5') were designed by primer-blast tool (www.ncbi.nlm.nih.gov/tools/primer-blast). The expression of the mentioned genes in cancer and normal samples was quantified using RT-qPCR with specific primers and SYBR Green. *GAPDH* (F: 3'-AAGCTCATTTCCTGGTATG-5' and R: 3'-CTTCCTCTTGTGCTCTTG-5') was utilized as an internal reference and $2^{-\Delta Ct}$ was used to calculate the expression of each gene in each sample.

Statistics and software

All initial preprocessing and data analysis were performed by the R programming language (V 4.0.2). GhraphPad (V 8) software was used to draw and display charts. The significance of candidate gene expression with patient prognosis was assessed using the LogRank test, with a logRank threshold of 0.05 being considered. Chi-square test was employed to investigate the association between the expression of candidate pseudogenes and clinical characteristics. Cytoscape (V 4) was employed to display the ceRNA network and the association of genes with identified pseudogenes.

Results

Dramatically changes in the expression of pseudogenes in GC

The expression differences among miRNAs revealed that 44 miRNAs increased and 42 miRNAs decreased (Fig. 1A, |logFC|>1 and FDR<0.01). Findings for differences in mRNA expression showed that 735 mRNA expression in cancer samples increased compared to normal and 1250 mRNA decreased (Fig. 1B, |logFC|>1 and FDR<0.01). However, while comparing the expression of pseudogenes in GC samples to normal samples, it was discovered that 23 pseudogenes had a significant increase in expression. In addition, the expression of 10 pseudogenes decreased significantly (Fig. 1C, |logFC|>1 and FDR<0.01).

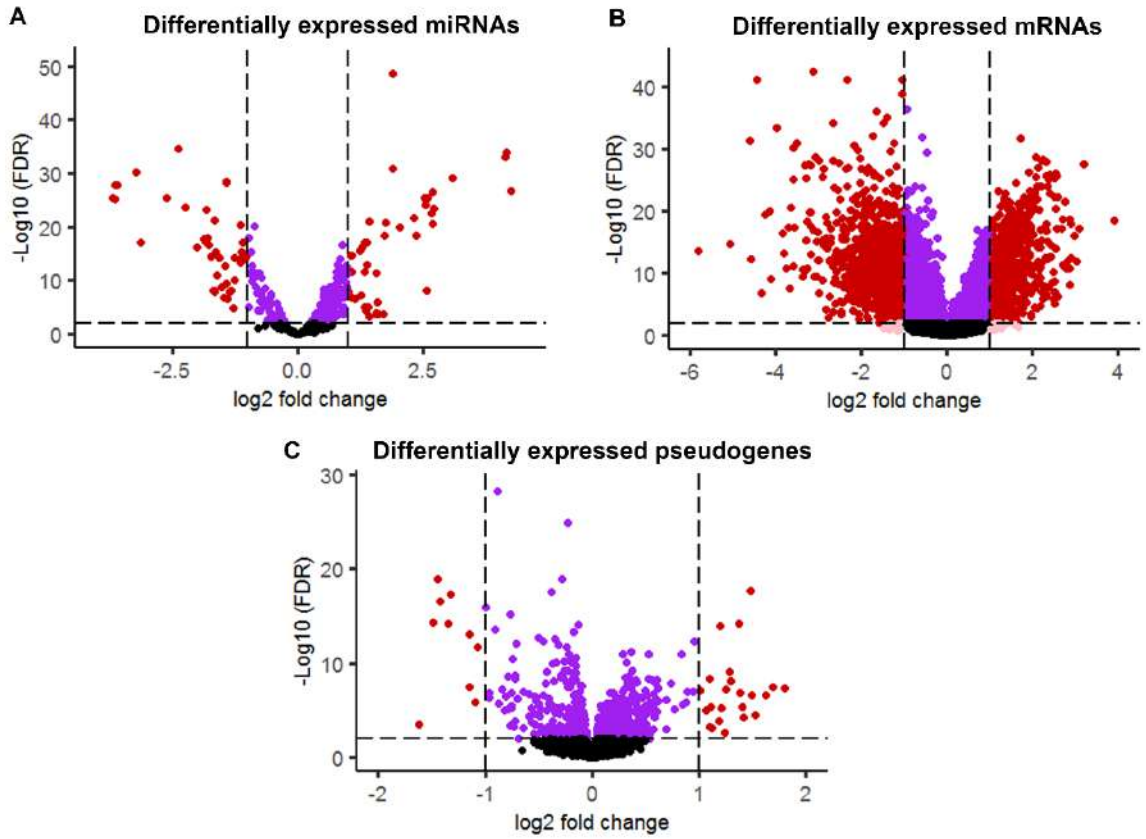

Fig. 1: The expression of many of pseudogenes in GC is significantly altered. (A-C) Expression differences for miRNAs, mRNA, and pseudogenes in cancer samples compared to normal are shown based on TCGA data. The

selection of genes was based on the |logFC|>1 and FDR<0.01 criteria (logFC; log fold change, FDR; false discovery rate)

RCN1P2, TPM3P9, and HSP90AB3P expression alterations in the development of GC via the ceRNA network

The results of combining miRNA-mRNA and miRNA-pseudogenes data are shown in Fig. 2A and supplementary Table 1. *RCN1P2*, *TPM3P9*, and *HSP90AB3P* had the highest connection and degree among other discovered pseudogenes with differentially expressed miRNAs in GC (Fig. 2A, blue nodes). Enrichment was also done to better understand the network-linked pathways, and the results revealed that many of the genes in the ceRNA network are involved in significant cancer cell pathways like cell proliferation (E2F Targets), mTORC1, metastasis (Epithelial Mesenchymal Transition), inflammation (TNF-alpha Signaling via NF-Kb and IL-2/STAT5 Signaling), Hypoxia, DNA repair (UV Response Dn and UV Response Up) and Hedgehog signaling (Fig. 2B, FDR<0.01).

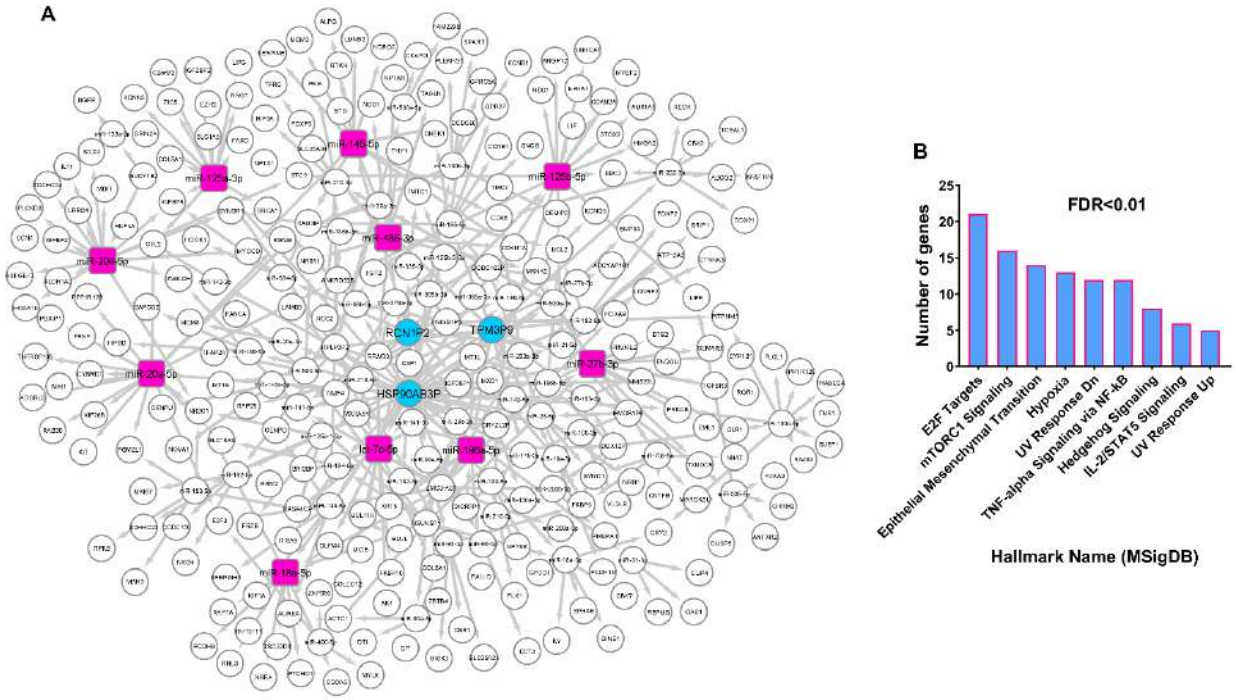

Fig. 2: *RCN1P2, TPM3P9*, and *HSP90AB3P* had the highest connection and degree among other discovered pseudogenes with differentially expressed miRNAs and mRNAs in GC. (A) The ceRNA network is shown based on miRNAs, mRNAs, and pseudogenes that had different expressions in GC. The blue nodes indicate the pseudogenes and the red nodes represent the miRNAs that have the highest degree in the network. **(B)** Enrichment results for all genes present in the ceRNA network

Association of RCN1P2 with cancer cell pathways and survival-related genes

RCN1P2 could bind to a total of 14 miRNAs, many of which target genes involved in key cancer cell pathways like proliferation, inflammation, and mTORC1 (Fig. 3A and C, FDR<0.01). TCGA data also show that *RCN1P2* expression is significantly increased in GC specimens compared to normal (Fig. 3B, logFC=1.7, FDR<0.01). Increased expression of *CCDC80*, *COLEC12*, *FKBP10*, and *NME4* genes was only related with poor prognosis among the genes in the *RCN1P2* network (Fig. 3D-G and logRank<0.05, Table 2). As outlined in Table S1,

the expression levels of *CCDC80*, *COLEC12*, *FKBP10*, and *NME4* demonstrate a notable increase in GC samples in comparison to healthy samples (logFC>1 and FDR<0.05). Additionally, the results of the network related to *RCN1P2* demonstrated that three miRNAs, namely miR-145-5p, let-7c-5p, and miR-125b-5p, exhibited the highest interactions with the mRNAs associated within the network (Fig .3A). The TCGA results indicate a decrease in the expression levels of these three miRNAs in GC (Table S1).

Table 2: The univariate Cox regression test results for candidate mRNAs in subnets

Variable	Univariate		
	HR	*P* value	95% CI
CCDC80 expression (High vs. Low)	1.48	0.004	1.12 – 1.95
COLEC12 expression (High vs. Low)	1.7	0.0001	1.3 – 2.3
FKBP10 expression (High vs. Low)	1.43	0.003	1.14 – 1.81
NME4 expression (High vs. Low)	1.6	0.0002	1.2 – 2.13
CYP1B1 expression (High vs. Low)	1.83	<0.0001	1.37 – 2.48
NPTX1 expression (High vs. Low)	1.39	0.001	1.13 – 1.71
NR3C1 expression (High vs. Low)	1.61	0.002	1.17 – 2.2
SNCG expression (High vs. Low)	1.52	0.0002	1.21 – 1.93
CLIP4 expression (High vs. Low)	1.4	0.008	1.09 – 1.9
GAS1 expression (High vs. Low)	1.5	0.001	1.17 – 1.9
KCNB1 expression (High vs. Low)	1.36	0.003	1.06 – 1.66
RNLS expression (High vs. Low)	1.38	0.004	1.1 – 1.74
SYNGR1 expression (High vs. Low)	1.49	0.002	1.15 – 1.93

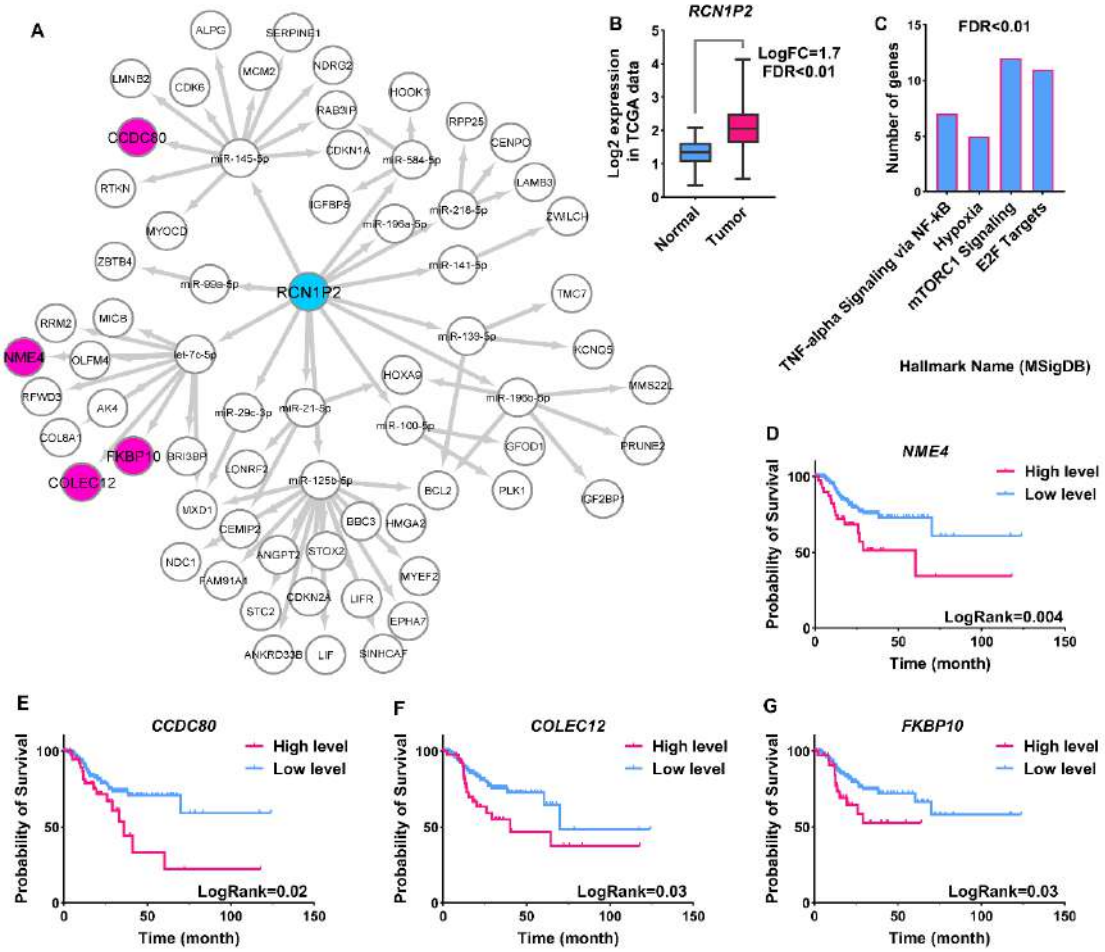

Fig. 3: The *RCN1P2*-regulatory network is linked to the primary pathways of cancer cells. (A) The subnet associated with *RCN1P2* is shown. **(B)** Differentially expressed *RCN1P2* in TCGA data is shown. **(C)** Enrichment results for all genes in the *RCN1P2* subnet. **(D-G)** Based on TCGA data, a Kaplan-Meier plot demonstrating the connection of gene expression in the *RCN1P2*-network with the prognosis of GC patients is shown

Increased expression of TPM3P9 associated with genes of inflammation, proliferation, and DNA repair pathways via the ceRNA network

The *TPM3P9* subnet revealed that this pseudogene interacts with 13 different miRNAs. These miRNAs can target 61 mRNAs significantly changed in GC (Fig. 4A). Based on TCGA data, *TPM3P9* expression in cancer samples was on average doubled compared to normal, as seen in Fig. 4B (logFC=1.1 and FDR<0.01). The results of *TPM3P9*-associated mRNA enrichment revealed that several of them are involved in inflammation, proliferation, and DNA repair pathways (Fig. 4C, FDR<0.01). *CCDC80*, *COLEC12*, *FKBP10*, and *NME4* genes (already linked to *RCN1P2* and associated with poor prognosis) were also linked to *TPM3P9*, but via various miRNAs (Fig. 4A). Our findings also revealed that in addition to the mentioned genes, the *TPM3P9* network included the *CYP1B1*, *NPTX1*, *NR3C1*, and *SNCG* mRNA, whose increased expression was linked to a bad prognosis in GC patients (Fig. 4D-G and logRank<0.05, Table 2). The previous results have demonstrated an increase in the expression levels of these mRNAs in GC samples compared to normal (Table S1). Moreover, within the network linked to *TPM3P9*,

the interactions with the associated mRNAs were notably prominent for five miRNAs: let-7c-5p, miR-210-3p, miR-27b-3p, miR-195-5p, and miR-222-3p (Fig .4A). The expression analysis of these miRNAs indicated a decrease in let-7c-5p, miR-27b-3p, and miR-195-5p levels, whereas hsa-mir-210-3p and hsa-mir-222-3p showed increased expression in GC (Table S1).

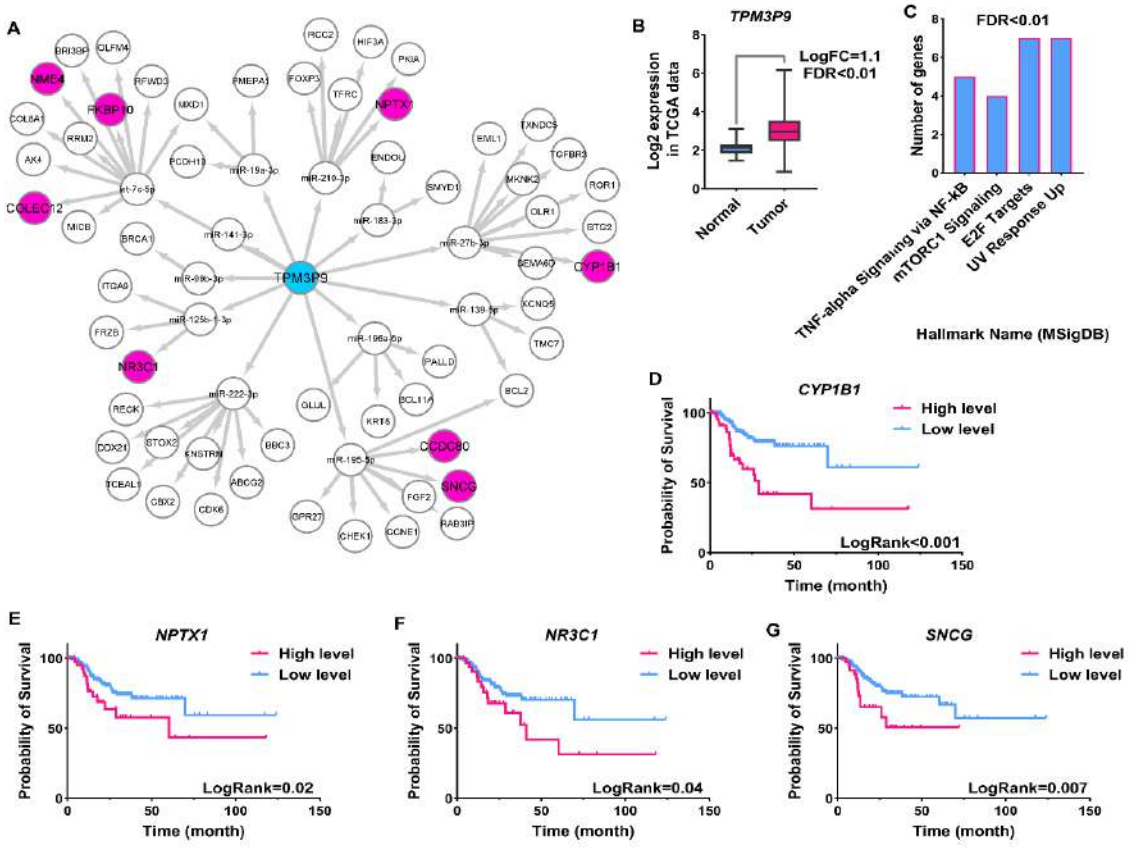

Fig. 4: The survival, proliferation, and inflammation genes are linked to the *TPM3P9* regulatory network. **(A)** The subnet associated with *TPM3P9* and all the genes in it is displayed. **(B)** The level of *TPM3P9* expression in cancer samples compared to normal based on TCGA data. **(C)** Pathways associated with *TPM3P9*-network genes is shown. **(D-G)** Relationship between the expression of candidate genes in the *TPM3P9* subnet and the survival rate of GC patients

Increased expression of HSP90AB3P with genes associated with metastasis in GC

The results of the *HSP90AB3P*-related subnet revealed that these pseudogenes interacted with 43 miRNAs. These miRNAs can also target 176 mRNAs with different expression patterns in GC (Fig. 5A). Examination of *HSP90AB3P* expression in TCGA data showed that its expression in cancer samples increased significantly compared to normal (Fig. 5B, logFC=1.4 and FDR<0.01). On the other hand, the enrichment results for *HSP90AB3P*-related mRNAs revealed that many of them are involved in cellular signaling pathways such as proliferation, inflammation, metastasis, DNA repair and hypoxia (Fig. 5C, FDR<0.01). The mRNAs identified for *RCN1P2* and *TPM3P9* that were linked to patient prognosis were also present in the *HSP90AB3P*-related ceRNA network (Fig. 5A). In addition, five genes including *CLIP4*, *GAS1*, *KCNB1*, *RNLS*, and *SYNGR1* in the *HSP90AB3P*-related network were present and their elevated expression was linked to poor patient prognosis (Fig. 5D-H, logRank<0.05, Table 2). The TCGA data indi-

cates a noticeable increase in the expression of the mentioned mRNAs in GC (Table S1). Moreover, within the network associated with *HSP90AB3P*, we identified eight miRNAs—let-7c-5p, miR-486-3p, miR-27b-3p, miR-130b-3p, miR-18a-5p, miR-20a-5p, miR-125a-3p, and miR-145-5p—that exhibited a higher degree compared to other miRNAs in the *HSP90AB3P* network (Fig .5A). Among the identified miRNAs, hsa-mir-130b-3p and hsa-mir-18a-5p exhibited increased expression, while the rest showed decreased expression in GC (Table S1). Interestingly, let-7c-5p was shared by all subnets.

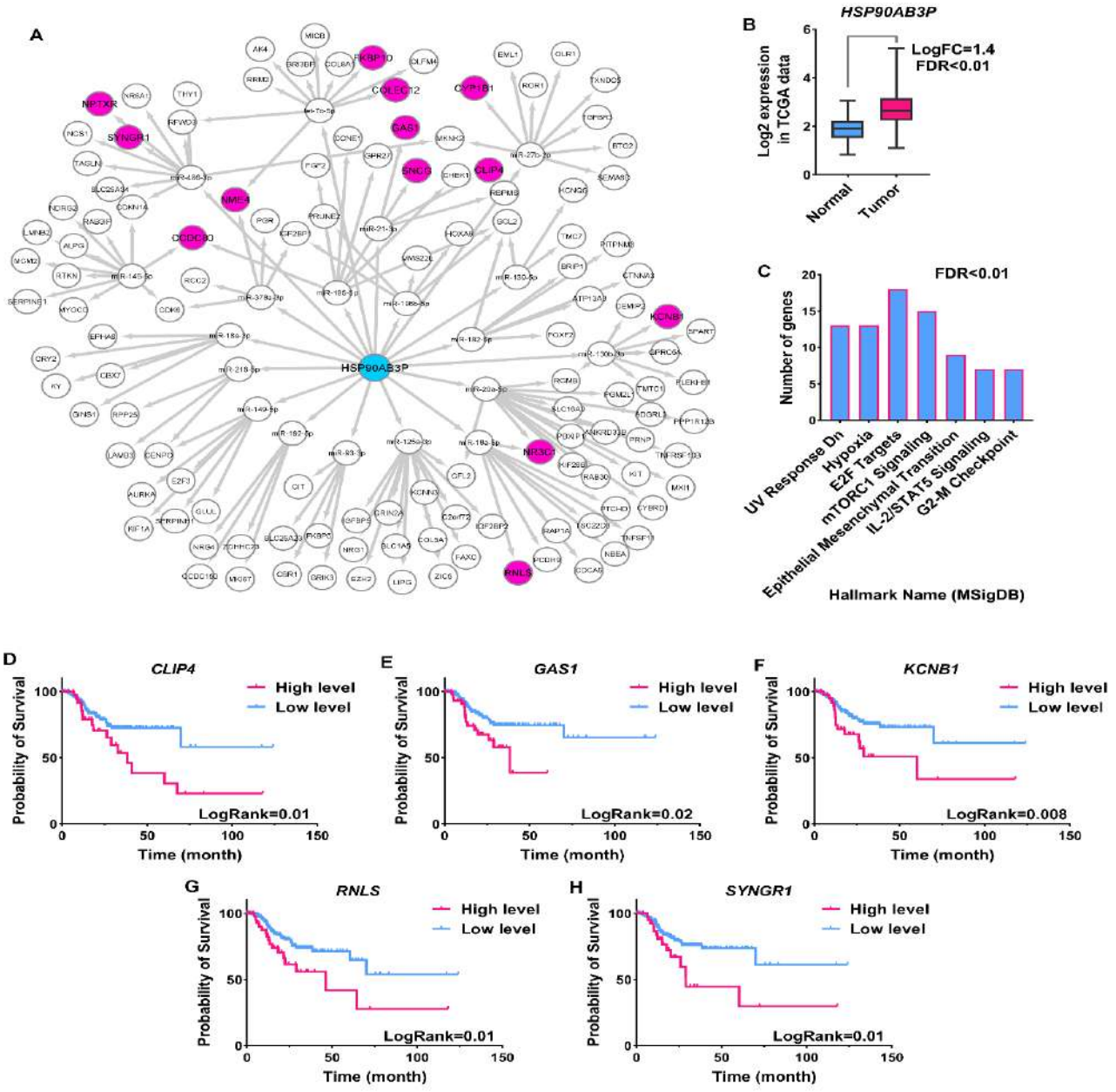

Fig. 5: The *HSP90AB3P* regulatory network regulates genes that are involved in the metastatic process. (A) *HSP90AB3P's* subnet is shown. (B) In the TCGA data, the difference in *HSP90AB3P* expression is noticeable. (C) Based on MSigDB data, enrichment findings for genes in the HSP90AB3P-regulatory network are calculated and displayed. (D-H) Correlation between expressions of candidate genes in *HSP90AB3P* network with patient survival rate

Up-regulated of RCN1P2, TPM3P9, and HSP90AB3P in GC samples compared to normal

The expression levels of *RCN1P2, TPM3P9*, and *HSP90AB3P* in GC samples were compared to normal adjacent samples using the RT-qPCR method to verify the findings. The results of *RCN1P2* expression showed that it rose significantly when compared to the normal level (Fig. 6A, $P<0.001$). *TPM3P9* expression was similarly shown to be considerably higher in cancer samples compared to normal samples in our research (Fig. 6B, $P<0.05$). Finally, RT-qPCR results for the expression level of *HSP90AB3P* revealed that the expression level of this gene increased dramatically in cancer samples (Fig. 6C, $P<0.0001$).

These findings support previous findings, demonstrating that *RCN1P2*, *TPM3P9*, and *HSP90AB3P* expression levels are much higher in GC and that they could have an oncogenic role in GC by modulating cell proliferation pathways, inflammation, and metastasis. We also investigated the relationship between the expression of the identified candidate pseudogenes and clinical characteristics, including age, gender, stage, TNM.T, TNM.N, and tumor location, based on the clinical data available in the TCGA database. The chi-square test results revealed no significant association between the expression levels of the identified candidate pseudogenes and various clinical characteristics such as age, gender, stage, TNM.T, TNM.N, and tumor location.

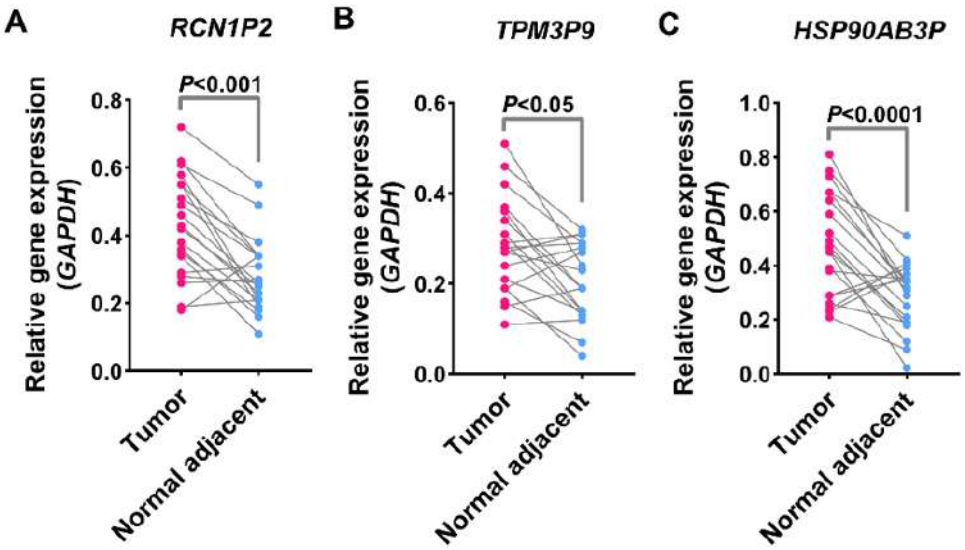

Fig. 6: *RCN1P2, TPM3P9*, and *HSP90AB3P* level is significantly increased in cancer specimens compared to normal based on RT-qPCR. (A-C) *RCN1P2*, *TPM3P9*, and *HSP90AB3P* expression are displayed in cancer samples compared to adjacent normal. $2^{-\Delta Ct}$ was used to calculate the expression of each gene in each sample

Discussion

Various studies have found that the expression of non-coding RNAs changes in various malignancies, including GC, and that these changes are related to malignancy and patient prognosis (15). As a result, discovering non-coding RNAs that can play a role in cancer development and progression can be beneficial and practical.

The results of this study showed for the first time that *RCN1P2* is increased in GC samples compared to normal and mRNAs associated with its subnet are involved in pathways such as proliferation, inflammation, and mTORC1. Furthermore, *CCDC80*, *COLEC12*, *FKBP10*, and *NME4* are linked to the regulatory network *RCN1P2*, with their expression levels elevated in GC. This elevation correlates with a worsened prognosis

for patients. *FKBP10* expression is increased in GC and is associated with poor prognosis in patients (16). Reduced *FKBP10* expression has been shown to lower malignancy in GC cell lines (17). *CCDC80* levels rise in GC and are correlated with a poor prognosis (18). Increased *COLEC12* expression in GC is associated with its aggressiveness (19). Our findings have demonstrated a potential interaction between *RCN1P2* and miR-145-5p, let-7c-5p, and miR-125b-5p, resulting in a significant decrease in the expression of these miRNAs in GC. MiR-145 has been shown in studies to suppress the proliferation, invasion, and migration of GC cell lines (20). Research indicates a significant decrease in the expression of miR-125b-5p, strongly associated with increased mortality rates (21). *RCN1P2* might play a role in the pathogenesis of GC by interacting with the mentioned miRNAs, which have tumor-suppressive roles. Pathways linked to the *RCN1P2* network, including proliferation, inflammation, and mTORC1, play a critical role in GC (22, 23).

TPM3P9 expression was elevated in GC samples, which could have an impact on the proliferation, inflammation, and survival-related genes via the ceRNA network. Genes including *CYP1B1*, *NPTX1*, *NR3C1*, and *SNCG*, associated with *TPM3P9*, show increased expression in GC, correlating with poor patient prognosis. Furthermore, our findings demonstrated an upregulation in *TPM3P9* expression in GC samples compared to normal tissues. *CYP1B1* can play a role in GC malignancy through boosting expression (24). *NPTX1* expression has been linked to poor prognosis, increased metastasis, and invasion, and it has been demonstrated to rise in GC (25). *SNCG* is elevated in GC and might be associated with increased invasiveness (26). Furthermore, our investigations demonstrated that let-7c-5p, miR-27b-3p, and miR-195-5p exhibit substantial interactions with the mRNAs associated with the ceRNA network of *TPM3P9*. The TCGA data indicated a significant downregulation in the expression of the mentioned miRNAs in GC. MiR-27b-3p undergoes modulation in GC and could play a significant role in suppressing the growth, invasion, and migration of GC cells (27). MiR-27b-3p decreases in GC and could potentially impact drug resistance (28). The results suggest that miRNAs associated with *TPM3P9* could play a significant role in GC. Perhaps *TPM3P9* might interfere with their function by acting as sponges to hinder their activity.

Our research found that *HSP90AB3P* expression was much higher in GC cancer samples based on TCGA and RT-qPCR data, and that it was linked to genes involved in metastatic pathways. *HSP90ABP* could also use the ceRNA network to regulate a number of genes linked to survival in GC patients, including *CLIP4*, *GAS1*, *KCNB1*, *RNLS*, and *SYNGR1*. Also, the mentioned genes showed increased expression in GC based on TCGA data. *CLIP4* is increased in GC and is associated with poor prognosis in patients (29). There are also reports indicating the involvement of *GAS1* and *KCNB1* in the pathogenesis of GC (30, 31). We have demonstrated that *HSP90AB3P* can interact with miRNAs such as let-7c-5p, miR-486-3p, miR-27b-3p, miR-20a-5p, miR-125a-3p, and miR-145-5p. Research has shown a reduction in miR-27b-3p levels in GC. This miRNA might contribute to the development of the disease by influencing genes associated with invasion and migration (32). Research has also shown a decrease in miR-145-5p levels in GC, potentially correlating with the survival rate of patients (33). These findings underscore the significance of *HSP90AB3P* in GC. Although more in vitro assays is needed, these findings imply that *RCN1P2*, *TPM3P9*, and *HSP90ABP* may have an oncogenic role in GC through influencing cancer cells' main pathways.

Conclusion

This study found elevated expression of *RCN1P2*, *TPM3P9*, and *HSP90ABP* pseudogenes in GC. Through computational analysis, these pseudogenes were shown to regulate pathways involved in metastasis, proliferation, and inflammation in GC.

Journalism Ethics considerations

Ethical issues (Including plagiarism, informed consent, misconduct, data fabrication and/or falsification, double publication and/or submission, redundancy, etc.) have been completely observed by the authors.

Conflict of Interests

The authors declare that there is no conflict of interest.

References

1. Sung H, Ferlay J, Siegel RL, et al (2021). Global cancer statistics 2020: GLOBOCAN estimates of incidence and mortality worldwide for 36 cancers in 185 countries. *CA Cancer J Clin*, 71(3):209-49.
2. Cho JY, Lim JY, Cheong JH, et al (2011). Gene expression signature–based prognostic risk score in gastric cancer. *Clin Cancer Res*, 17(7):1850-7.
3. Dorosti S, Jafarzadeh Ghoushchi S, Sobhrakhshankhah E, et al (2020). Application of gene expression programming and sensitivity analyses in analyzing effective parameters in gastric cancer tumor size and location. *Soft Computing*, 24(13):9943-64.
4. Yasui W, Oue N, Aung PP, et al (2005). Molecular-pathological prognostic factors of gastric cancer: a review. *Gastric Cancer*, 8(2):86-94.
5. Chawla S, Rockstroh A, Lehman M, et al (2022). Gene expression based inference of cancer drug sensitivity. *Nat Commun*, 13(1):5680.
6. Tyner JW, Haderk F, Kumaraswamy A, et al (2022). Understanding drug sensitivity and tackling resistance in cancer. *Cancer Res*, 82(8):1448-60.
7. Sisu C (2021). Pseudogenes as Biomarkers Biomarkers and Therapeutic Targets Therapeutic targets in Human Cancers. *Methods Mol Biol*, 2324:319-337.
8. Xiao-Jie L, Ai-Mei G, Li-Juan J, et al (2015). Pseudogene in cancer: real functions and promising signature. *J Med Genet*, 52(1):17-24.
9. Hayashi H, Arao T, Togashi Y, et al (2015). The OCT4 pseudogene POU5F1B is amplified and promotes an aggressive phenotype in gastric cancer. *Oncogene*, 34(2):199-208.
10. Guo X, Deng L, Deng K, et al (2016). Pseudogene PTENP1 suppresses gastric cancer progression by modulating PTEN. *Anticancer Agents Med Chem*, 16(4):456-64.
11. Emadi-Baygi M, Sedighi R, Nourbakhsh N, et al (2017). Pseudogenes in gastric cancer pathogenesis: a review article. *Brief Funct Genomics*, 16(6):348-60.
12. Ma H, Ma T, Chen M, et al (2018). The pseudogene-derived long non-coding RNA SFTA1P suppresses cell proliferation, migration, and invasion in gastric cancer. *Biosci Rep*, 38(2):BSR20171193.
13. Ye J, Li J, Zhao P (2021). Roles of ncRNAs as ceRNAs in Gastric Cancer. *Genes (Basel)*, 12(7):1036.
14. Zhang R, Guo Y, Ma Z, et al (2017). Long non-coding RNA PTENP1 functions as a ceRNA to modulate PTEN level by decoying miR-106b and miR-93 in gastric cancer. *Oncotarget*, 8(16):26079-26089.
15. Ghafouri-Fard S, Taheri M (2020). Long non-coding RNA signature in gastric cancer. *Exp Mol Pathol*, 113:104365.
16. Liang L, Zhao K, Zhu JH, et al (2019). Comprehensive evaluation of FKBP10 expression and its prognostic potential in gastric cancer. *Oncol Rep*, 42(2):615-28.
17. Wang RG, Zhang D, Zhao CH, et al (2020). FKBP10 functioned as a cancer-promoting factor mediates cell proliferation, invasion, and migration via regulating PI3K signaling pathway in stomach adenocarcinoma. *Kaohsiung J Med Sci*, 36(5):311-7.
18. Li X, Du Y (2024). Lactate metabolism subtypes analysis reveals CCDC80 as a novel prognostic biomarker in gastric cancer. *J Cancer*, 15(17):5557-5576.
19. Kong W, Wang Z, Wang B (2023). Unveiling DNA damage repair-based molecular subtypes, tumor microenvironment and pharmacogenomic landscape in gastric cancer. *Front Genet*, 14:1118889.
20. Qiu T, Zhou X, Wang J, et al (2014). MiR-145, miR-133a and miR-133b inhibit proliferation, migration, invasion and cell cycle progression

via targeting transcription factor Sp1 in gastric cancer. *FEBS Lett*, 588(7):1168-77.
21. Li G, Ao S, Hou J, et al (2019). Low expression of miR-125a-5p is associated with poor prognosis in patients with gastric cancer. *Oncol Lett*, 18(2):1483-90.
22. Hibdon ES, Razumilava N, Keeley TM, et al (2019). Notch and mTOR signaling pathways promote human gastric cancer cell proliferation. *Neoplasia*, 21(7):702-12.
23. Jaroenlapnopparat A, Bhatia K, Coban S (2022). Inflammation and gastric cancer. *Diseases*, 10(3):35.
24. Cheng H, Sharen G, Wang Z, et al (2021). LncRNA UCA1 enhances cisplatin resistance by regulating CYP1B1-mediated apoptosis via miR-513a-3p in human gastric cancer. *Cancer Manag Res*, 13:367-377.
25. Yan H, Zheng C, Li Z, et al (2019). NPTX1 promotes metastasis via integrin/FAK signaling in gastric cancer. *Cancer Manag Res*, 11:3237- 3251.
26. Zheng S, Shi L, Zhang Y, et al (2014). Expression of SNCG, MAP2, SDF-1 and CXCR4 in gastric adenocarcinoma and their clinical significance. *Int J Clin Exp Pathol*, 7(10):6606-15.
27. Chen X, Cui Y, Xie X, et al (2018). Functional role of miR-27b in the development of gastric cancer. *Mol Med Rep*, 17(4):5081-7.
28. Nie H, Mu J, Wang J, et al (2018). miR-195-5p regulates multi-drug resistance of gastric cancer cells via targeting ZNF139. *Oncol Rep*, 40(3):1370-1378.
29. Wang G, Zhan T, Li F, et al (2021). The prediction of survival in Gastric Cancer based on a Robust 13-Gene Signature. *J Cancer*, 12(11):3344- 3353.
30. Farah A, Kabbage M, Atafi S, et al (2020). Selective expression of KCNA5 and KCNB1 genes in gastric and colorectal carcinoma. *BMC Cancer*, 20: 1179.
31. Zhong Q, Wang HG, Yang JH, et al (2023). Loss of ATOH1 in Pit Cell Drives Stemness and Progression of Gastric Adenocarcinoma by Activating AKT/mTOR Signaling through GAS1. *Adv Sci (Weinh),* 10(32):e2301977.
32. Bao C-h, Guo L (2022). miR-27b-3p inhibits invasion, migration and epithelial-mesenchymal transition in gastric cancer by targeting RUNX1 and activation of the hippo signaling pathway. *Anticancer Agents Med Chem,* 22(5):864-873.
33. Zhang Y, Wen X, Hu X, et al (2016). Downregulation of miR-145-5p correlates with poor prognosis in gastric cancer. *Eur Rev Med Pharmacol Sci*, 20(14):3026-30.